Properties of short polystyrene chains confined between two Gold surfaces through a combined Density Functional Theory and classical Molecular Dynamics approach

Karen Johnston and Vagelis A. Harmandaris

Properties of Short Polystyrene Chains Confined Between two Gold Surfaces Through a Combined Density Functional Theory and Classical Molecular Dynamics Approach.

Karen Johnston,[*,†] Vagelis Harmandaris,[*,‡] and Kurt Kremer ??[*,†]

Max-Planck Institute for Polymer Research, P.O. Box 3148, Mainz 55021, Germany, and Department of Applied Mathematics, University of Crete GR-71409 Heraklion, Crete, Greece and IACM FORTH GR-71110 Heraklion

E-mail: johnston@mpip-mainz.mpg.de; vagelis@tem.uoc.gr; kremer@mpip-mainz.mpg.de

Abstract

The properties of atactic short-chain polystyrene films confined between two parallel gold surfaces at a temperature of 503 K are investigated through detailed DFT calculations and classical atomistic simulations. A new classical Morse-type potential, used to describe the interaction between the polymer and the gold surface, was parameterized based on the results of density functional calculations. Several polystyrene films were studied, with thicknesses ranging from around 1.2 nm to 10 nm. The structural, conformational and dynamical properties of the films were analysed and compared to the properties of the bulk polystyrene systems. The dynamics of the polystyrene close to the surface was found to be significantly slower than in the bulk.

[*]To whom correspondence should be addressed

[†]Max-Planck Institute for Polymer Research, P.O. Box 3148, Mainz 55021, Germany

[‡]Department of Applied Mathematics, University of Crete GR-71409 Heraklion, Crete, Greece and IACM FORTH GR-71110 Heraklion

Introduction

The study of hybrid polymer/solid interfacial systems at the molecular level is a very intense research area due to the development of composite materials, coatings, etc. The properties of confined macromolecules can be radically different from the bulk properties. For example, for polymer thin films on a substrate it was found that the glass transition temperature, T_g, decreases with decreasing film thickness.[? ? ? ? ?] This decrease in T_g is attributed to the increased mobility of the chains at the free surface. This observation is supported by molecular dynamics (MD) simulations[? ?] which have observed greater mobility at the free surface.

Conversely, MD simulations observe a slowing down of the dynamics at the solid surface.[? ? ? ?] So far, experiments have not been able to directly analyse the effect of the solid surface on the properties/dynamics of the polymer and T_g is, therefore, an average over the entire film. While MD simulations have also been used to measure the glass transition temperature,[? ?] these simulations were carried out using a structureless wall potential to model the solid surface. The effect of corrugation in the surface potential is crucial as demonstrated in a study of polycarbonate on a silicon surface, which showed that a smooth surface potential results in faster dynamics than in bulk whereas the introduction of a site-dependence to the surface potential dramatically slows the polymer dynamics.[?]

Furthermore, simulation studies of macromolecular liquids near solid surfaces have addressed issues related to the structure and dynamics of polymer melts confined between two impenetrable plates. In off-lattice dynamic Monte Carlo simulations[? ? ?] and stochastic dynamics simulations,[?] the wetting behaviour of thin polymer films,[? ?] the behaviour of n-alkane films of various thickness adsorbed on a crystalline substrate [modelling Au(001) crystal],[?] and aspects of structural relaxation and dynamic heterogeneity in a polymer melt at flat and structured surfaces[? ? ?] Moreover, dynamics of polymer/solid interfacial systems have been also studied through molecular simulations with atomistic[? ?] and bead-spring[? ?] models as well as with MC simulations using the bond fluctuation model.[?]

Overall, the structure and dynamics of a polymer at a surface depends on the chemistry of the

polymer and the surface. Many MD studies take forcefield parameters from molecule–molecule interactions and apply these to studies of molecules on surfaces, even though the chemical environment is quite different. However, to obtain quantitative information from MD simulations it is essential that the classical potential accurately describes the interaction between the specific molecule and surface of interest. In order to achieve this, a more reliable procedure is to construct classical potentials based on detailed quantum calculations. Since it is computationally impossible to simulate a large macromolecule at a surface using quantum mechanical methods, a frequent approach is to divide the macromolecule into submolecules. This approach has been used in other systems, for example, $C_52H_72O_3$ on TiO_2 [?] and bisphenol-A-polycarbonate on Ni(111) [?] and Si(001)-(2×1). [?]

In this paper we focus on the structural and dynamical properties of atactic short–chain polystyrene (PS) films between two Au(111) surfaces. To quantitatively study PS/Au systems we use a dualscale modelling approach that involves detailed density functional theory (DFT) calculations and classical MD simulations of PS/Au systems. Au(111) has a well-defined surface structure, compared to substrates such as silica, which makes it easier to understand the interaction between the polymer and the surface. The interaction of one styrene monomer with gold is assumed to be well represented by the interactions of its two components (benzene and ethane) with gold. Parameters of the atomistic pair potentials for the surface interaction are obtained by fitting the classical molecule–surface interaction to the equivalent interaction calculated using DFT with van der Waals forces. The development of a classical surface potential based on the DFT results is described and the accuracies of Lennard–Jones and Morse potentials are compared. For the benzene–gold interaction we use previously parameterised Morse potentials. [?] Finally, the properties of atactic styrene oligomers films of different thicknesses confined between two parallel gold surfaces are investigated.

In the next section we describe the methodology giving some details about the DFT calculations as well as the classical atomistic MD simulations. In section 3 we present results from the DFT calculations of ethane on the Au(111) surface. The new PS/Au classical force field, derived through

an optimization procedure of the DFT data, is described in Section 4. The analysis of the density, structure and dynamics of various PS/Au systems are given in section 5. Finally, our findings and conclusions are summarized in Section 6. Must check numbering at the end!

Method

Density functional theory (DFT) calculations were performed using the VASP code,[? ? ? ?] which employs a plane wave basis set to describe the valence electrons. A plane wave cutoff energy of 400 eV was chosen and projected augmented waves were used to describe the core electrons.[? ?] van der Waals interactions were included via a self-consistent implementation of the vdW-DF functional[? ? ?] with PBE exchange.[? ?] The calculated lattice constant of bulk, fcc Au was 4.23 Å a value that overestimates the experimental one of $a_0 = 4.08$ Å by less than 4%. For the adsorption calculations, the surface was 4×4 times the surface unit cell, which corresponds to a coverage of 0.0625 monolayers. This was sufficient to avoid any interaction between the molecule and its periodic image. A Brillouin zone mesh of $4 \times 4 \times 1$ was used (equivalent to $16 \times 16 \times 1$ for a surface unit cell). The relaxations were terminated when the maximum force on any atom was less than 10 meVÅ^1.

The classical atomistic MD NPT simulations were performed using the GROMACS code.[? ? ?] The pressure was maintained at $p = 1$ atm using a Berendsen barostat. The stochastic velocity rescaling[?] thermostat was used to keep $T = 503$ K. A time step of 0.001 ps was used. In the classical simulations the surface is represented by an array of fixed particles placed in the ideal positions of bulk gold. For the classical simulations the experimental lattice constant, $a_0 = 0.408$ nm, of gold at T=300 K was used. This keeps the current ethane–gold potential consistent with the previously developed forcefield for benzene–gold. Furthermore, gold has a very small thermal expansion and only increases to 0.410 nm at $T = 618$ K.[?] Periodic boundary conditions were used in all directions so that the PS also interacts with the bottom of the gold surface in the image cells. The electrostatics are summed in the x and y directions only. A 7-atomic-layer slab with a

thickness of the $\approx$ 1.65 nm was used, which is thicker than the vdW cutoff length of 1.0 nm. The atomistic force field parameters for PS were taken from literature[?] and arithmetic combination rules were used. The reference bulk PS system consists of 50 10-monomer chains in a cubic box. The force field between the phenylene C and H atoms and gold was taken from a study of benzene on gold[?] and the force field for the C and H backbone atoms is fitted to the DFT results for ethane on gold as described below.

Four films, denoted S1 to S4, with different numbers of chains, N, were prepared. The chains were all 10 monomers long ($M_W = 1040$ g mol^{-1}) and each chain has a random tacticity. For the thicker films, S3 and S4, the lateral dimension of the surface is a=4.616 nm, corresponding to 16$\times$16 surface unit cells along the a and b directions (see Figure 1). For the thinnest two films the surface was doubled in x and y (32$\times$32 surface unit cells) to improve statistics.

The PS/Au systems were set up and equilibrated as follows. First, chains with different tacticities were set up in an hexagonal box with a gold slab and run with pressure coupling in the z-direction at 1 atm. The systems were equilibrated by running at a high temperature T_{equil} for 10 ns after which the end-to-end vector is decorrelated. This was followed by cooling to the target temperature of 503 K. Cooling rates of 10-300 K/ns were tested and the dependence of the properties on the cooling rate was checked. Afterwards, a cooling rate of 25-30 K/ns was chosen and once the temperature reached 503 K the system was run for some extra time before statistics were taken. Finally, after equilibration production runs were performed, of 100 ns duration. The equilibration temperatures, T_{equil}, and cooling rates, τ, are given in Table 1. For the smallest system three independent films were prepared.

Table 1: Setup and equilibration details for the four films.

System	N	T_{equil} (K)	τ (K/ns)
S1A	40	1200	25
S1B	40	1200	25
S1C	40	1200	25
S2	80	1000	25
S3	50	800	30
S4	100	800	30

Results and Discussion

In this section we present results about the confined PS systems from the detailed DFT calculations and the classical atomistic simulations.

Density functional theory

The main usage of the DFT calculations is to study the (single) monomer/surface interaction and also to derive an accurate and reliable classical atomistic force field for the molecule(PS)/surface(Au) interaction. As mentioned in the introduction, the interaction of one styrene monomer with gold is assumed to be well represented by the interactions of its two components (benzene and ethane) with gold. Parameters for the benzene/Au interaction are taken from a previous parametrization of DFT calculations.[?] Here we calculate parameters for the ethane/Au interaction.

There are three adsorption sites for ethane on the Au(111) surface, namely, the top site (T), the bridge site (B), and the hollow sites (H)[1] as shown in Figure 1. In order to study the (many) possible orientations for ethane on the surface we define θ as the angle that the C–C bond makes with the surface plane and ϕ as the angle between the C–C bond and any crystallographic (100) direction as shown in Figure 1. We refer to orientations with $\theta = 0$ as flat and with $\theta = 90$ as vertical. We define the adsorption energy as $E_{\text{ads}} = E_{\text{mol}} + E_{slab} - E_{\text{tot}}$ where E_{tot}, E_{mol} and E_{slab} are the total energies of the whole system, the ethane molecule and the gold surface slabs, respectively. The distance z is defined from the ethane molecule center-of-mass to the first-top Au layer (see Figure 1b). θ is the angle between the C–C bond of the ethane and the z axis, whereas ϕ is the angle between C–C bond and a-axis.

The adsorption energies for each site and various orientations are shown in Table 2. The ground state configuration is on the hollow site with $\theta = 0^{\text{o}}$, $z = 3.51$ Å and an adsorption energy of 35.7 kJ mol^{-1}. The dependence on the adsorption site is weak with differences in adsorption energy of about $2-3\%$, which is similar to the behaviour observed for benzene on Au(111).[?]

[1]There two hollow sites on Au(111), namely fcc and hcp, but since the difference in energy between them is so small we will just refer to them as hollow sites.

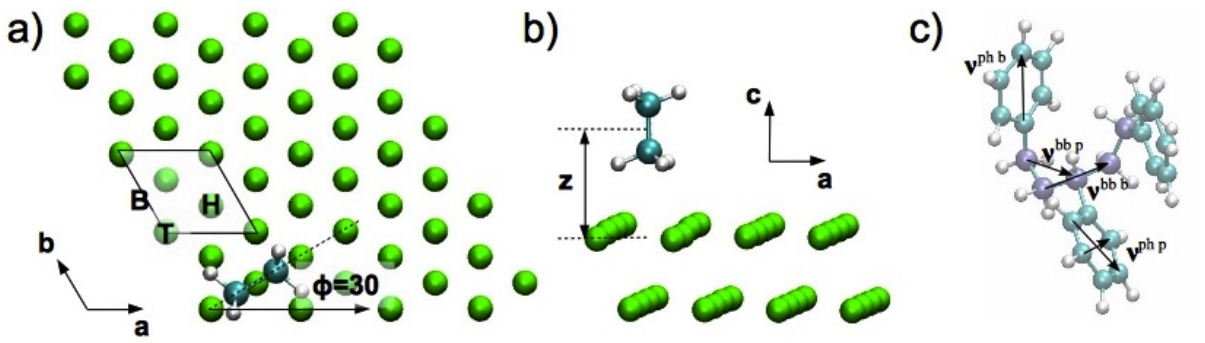

Figure 1: a) The Au(111) surface showing an ethane molecule on a hollow site, H, oriented with angle $\theta = 0$ (C–C bond flat on the surface) and $\phi = 30$ (angle between C–C bond and a-axis. The T, B and H show where the centre of the molecule would be for top, bridge and the second hollow sites, respectively. b) The ethane molecule on the H site with $\theta = 90$. z is defined as the perpendicular distance between the mid-point of the C atoms and the ideal position of the top Au atoms.

In contrast there are clear differences between the adsorption energies of the different molecule orientations i.e. E_{ads} of the vertical configurations ($\theta = 90^{\text{o}}$) is about 20% less than the flat ones for all sites. However, the dependence on the in–plane angle ϕ is very weak.

The interaction between ethane and gold is not as well studied as the interaction between benzene and gold. The reason is that the interaction between alkanes and metal surfaces is mostly due to van der Waals forces and only recently accurate vdW functionals for DFT calculations have been developed.?? If we calculate the more specific: ground state structure using the PBE functional with the corresponding equilibrium gold lattice constant of 4.17 Å the adsorption energy is only 9.6 kJ mol^{-1}. Similar behaviour was also seen for other molecules that do not form strong chemical bonds with the surface as, for example, benzene adsorbed on gold.? (VH: Do we know of any other systems?). SAMs, thiols: Thiols form a chemical bond with Au. ?? As far as we are aware, there is only one experimental study for the adsorption energy of ethane on gold, which used ..., and found an adsorption energy of 24.1 kJ mol^{-1}.? Our calculations give a larger adsorption energy, which is not surprising and has been also observed for other molecule/surface systems.?? The cause of such discrepancies between the DFT calculations and experimental data are related with inaccuracies in the DFT level (mainly the specific choice of the PBE exchange functional)

as well as with the experimental uncertainties related to deviations from a perfect crystal (surface roughness), impurities, etc.

Table 2: Adsorption sites, angles, distances and energies for ethane with 0.0625 ML coverage.

Site	θ (°)	ϕ (°)	z (Å)	E_{ads} (kJ mol^{-1})
H	0	0	3.51	35.7
H	0	30	3.51	35.7
H	90	0	4.10	28.9
H	90	30	4.10	28.0
T	0	0	3.66	34.7
T	90	0	4.25	27.0
B	0	0	3.51	34.7
B	90	0	4.10	28.0

Classical force field for the PS/Au interaction

A major part of the current work concerns the development of an accurate force field for the polymer/surface interaction. This is of particular importance since the strength of the adhesive energy determines the properties of the hybrid interfacial system. A standard approach in many classical simulations, is to use force fields for surface interactions that were parametrized for the bulk material rather than interfacial systems or which used DFT calculations that neglected vdW forces. However, as shown in the previous subsection, the vdW forces are substantial and should not be ignored for typical polymer/solid systems, including the PS/Au system studied here. Thus, in order to develop an accurate classical force field, we use the data from the DFT calculations presented in the previous section. In more detail we try to obtain, through an optimization procedure, a set of classical atomistic non-bonded pair parameters that describe *all* available DFT data. Note that this approach has successfully used for describing benzene/Au systems.[?]

As mentioned above, for the classical simulations we use a detailed model in which all surface Au atoms are presented explicitly. Then, we obtain pair potentials for the molecule–surface interaction (in our case Au-C and Au-H) using the detailed DFT data. Different functional forms can be used for the classical pair intermolecular potentials and in this work we considered two of them.

The first is the Lennard-Jones pair potential

$$V_{\mathrm{LJ}}(r) = \varepsilon_{i,j}\left\{\left(\frac{\sigma_{i,j}}{r_{i,j}}\right)^{12} - \left(\frac{\sigma_{i,j}}{r_{i,j}}\right)^{6}\right\} \tag{1}$$

which has two adjustable parameters, $\varepsilon_{i,j}$ and $\sigma_{i,j}$, per atom pair. The second is a more detailed Morse-type pair potential of the form

$$V_{\mathrm{M}}(r) = \varepsilon_{i,j}\left\{\exp\left[-2\alpha_{i,j}(r_{i,j} - r_{0i,j})\right] - 2\exp\left[-\alpha_{i,j}(r_{i,j} - r_{0i,j})\right]\right\} \tag{2}$$

which has three adjustable parameters, $\varepsilon_{i,j}$, $r_{0i,j}$ and $\alpha_{i,j}$, per atom pair, where the parameter α determines the shape/width of the potential. For both potentials the indices i and j denote the atom types (in this case i is an Au atom and j is a C or H atom).

Our goal is to find the set of non-bonded parameters that best describe all the available DFT data, i.e. molecule/surface interaction energies for different adsorption sites, molecule orientations and over a suitable range of molecule–surface distances, z. This is a complicated numerical problem, since it involves fitting over a many-parameter space without a clear global minimum. To achieve this we use an optimization algorithm, which is based on simulated annealing. In this scheme the parameters of the molecule/surface non-bonded interaction are determined iteratively (starting from an initial guess) in order to minimize a target-cost function. The cost function is defined as the difference between the quantum and classical molecule–surface interaction energies, for all distances and all different configurations (various adsorption sites and orientations). More details about the optimization scheme can be found elsewhere.[?]

A PS monomer consists of C and H backbone atoms as well as C and H atoms of the phenylene group, as shown in Figure 1c. For the latter we use the force-field developed previously for describing benzene–gold systems.[?] For the former, we use the DFT data obtained for ethane (see previous section) to develop new ethane–gold surface potentials, in a similar procedure as used for benzene on gold. The fitting procedure uses the data for all three sites, H, B and T, with both flat and vertical orientations. Since the dependence on ϕ is negligible we only considered orientations

with $\phi = 0$. In Figure 2 the DFT data for the various molecule orientations (squares for the flat and circles for the vertical ones) as well as the results from the classical pair potentials (lines), taken from the optimization procedure described above, are shown. Optimised parameters for the pair atomistic interactions are given in Table 3.

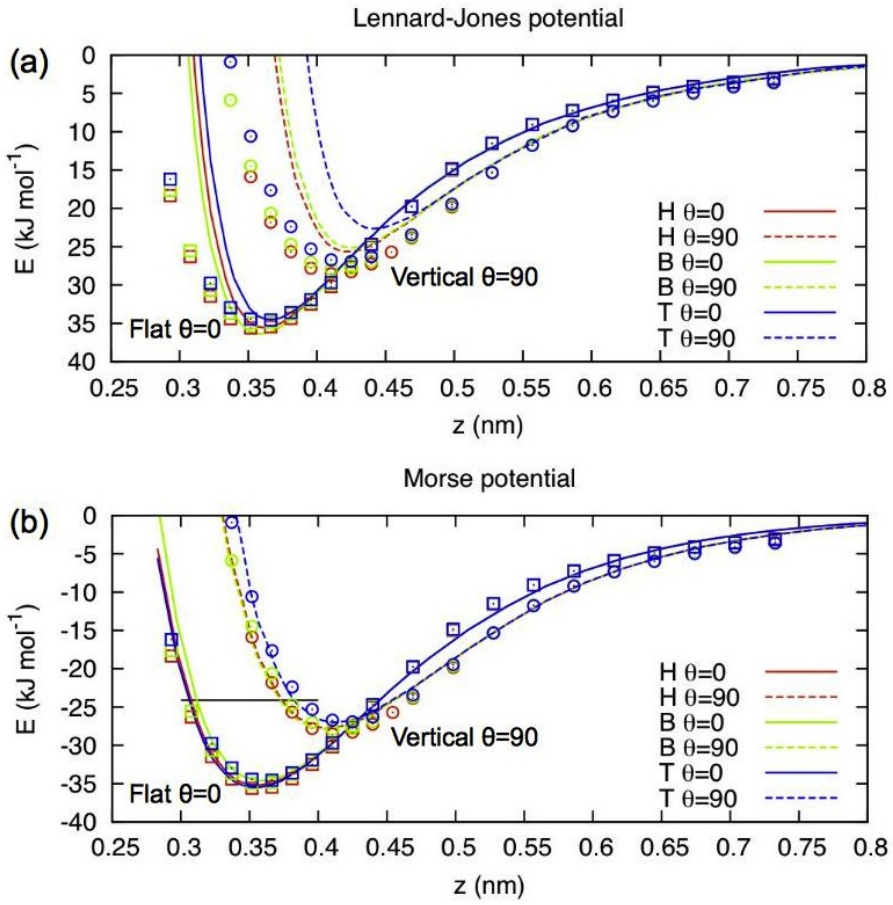

Figure 2: Adsorption energy as a function of the distance from the surface. The DFT results (symbols) are compared to the results from the pair potentials (lines), obtained from the optimization procedure using (a) Lennard-Jones and (b) Morse non-bonded potentials.

First, in Figure 2a we present classical molecule–surface interactions using the standard LJ potentials compared to DFT. It was not possible to find a set of LJ parameters that describe all the DFT minima simultaneously, thus the classical data were obtained by parameterizing each adsorption site, for the flat configurations, independently. Furthermore, it is also not possible to find a set of parameters that fit all the points (different molecule–surface distances) for a specific

Table 3: Force field parameters for the interaction of PS with the Au(111) surface. The parameters for the phenylene atoms were taken from Ref.[?]

Type	Atom pair	σ(nm), r_0(nm)	ε (kJ/mol)	α (nm^{-1})
LJ	Au-C_{ethyl}	0.37	1.95	-
LJ	Au-H_{ethyl}	0.25	0.16	-
Morse	Au-C_{ethyl}	0.42	0.95	12.06
Morse	Au-H_{ethyl}	0.38	0.42	9.74
Morse[?]	Au-C_{phenyl}	0.41	0.93	10.14
Morse[?]	Au-H_{phenyl}	0.40	0.31	11.66

configuration. IS THIS TRUE? Which site is shown in Fig2a? In Fig2a we show all three flat sites For the flat configurations, the classical interaction at the minima and longer distances are in a rather good agreement with the DFT data, although the shape of the interaction curve is too steep at low values of z. To check the transferability of the obtained classical potential parameters we use them to calculate the molecule–surface interaction energy of the vertical configurations (dashed lines in Figure 2a. It is also clear that there are strong deviations between the derived classical energies and the DFT data in all but the large molecule-surface distances. The reason for these discrepancies is most probably found in the very steep form of the repulsive part (12th power) of the LJ potential, which is not suitable for describing the complex short-range quantum behaviour of the molecule–surface system, related to electronic overlap and relaxation.

In the second parameterization we have used a non-bonded Morse-type potential for the classical pair C-Au and H-Au interaction. We fit simultaneously both the flat and the vertical molecule orientations. Results are shown in Figure 2b. In contrast to the LJ data discussed above, the optimization scheme using the Morse potential (data in Figure 2b) works much better; i.e. data from atomistic classical simulations can accurately describe the DFT data for *all* different molecule orientations and molecule/surface distances studied here. It is also interesting to note the very good agreement between the classical and the DFT data even for very short molecule-surface distances, where there are small displacements of the Au atoms from their ideal postitions (see Figure 1b), which are not described at the classical level.

In summary, it is clear that a classical atomistic pair parameterization of the PS/Au interac-

tion using a Morse-type potential is better than the Lennard-Jones one in describing the DFT data. Finally, we should also state that a Lennard-Jones potential was previously used to describe the interaction between organic molecules and surfaces by fitting to DFT and second-order Møller-Plesset calculations.[?] However, no direct comparison between the *ab initio* results and the Lennard-Jones potentials was presented. Our data show clearly that typical LJ pair potentials for the molecule–surface interaction cannot accurately describe the DFT data for the whole range of molecule–surface distances.

Confined Polystyrene Films

In this section we present results from classical atomistic MD simulations of PS confined systems, using the new PS/Au atomistic interaction developed in the previous section. We have simulated four different systems, S1–S4, (see Table 1) with 40, 80, 50 and 100 PS oligomers, respectively, between two parallel Au(111) surfaces. For the smallest system, which is the most strongly confinement, we have performed three independent simulations, to check the dependence on setup and history of the samples. In all cases T=503 K and P=1 atm. In Figure 3 we present typical snapshots, taken from the MD simulations, for each film. From these snapshots a PS adsorption layer can be seen at the Au surfaces for all systems.

Structural properties

Various properties of the different systems, including film thickness, d, density, ρ, average end-to-end distance, $< R_{\mathrm{e}}^2 >^{\frac{1}{2}}$, and radius of gyration, $< R_{\mathrm{g}}^2 >^{\frac{1}{2}}$, are presented in Table 4. The film thicknesses were calculated by subtracting the thickness of the 7-atomic-layer gold slab (where the interlayer spacing of Au(111) is $a_0/\sqrt{3} = 1.65$ nm) from the average box length along the z-direction. The average film thicknesses of the four model systems are approximately 0.96 nm, 1.9 nm, 4.8 nm and 9.8 nm, which correspond to about 0.62, 1.2, 3.1 and 6.4 times the average end-to-end distance ($< R_{\mathrm{e}}^2 >^{\frac{1}{2}} = 1.54$ nm) of 10-mer bulk PS, respectively. The average density in each case is higher than the bulk density, which is due to the denser adsorption layer at the gold

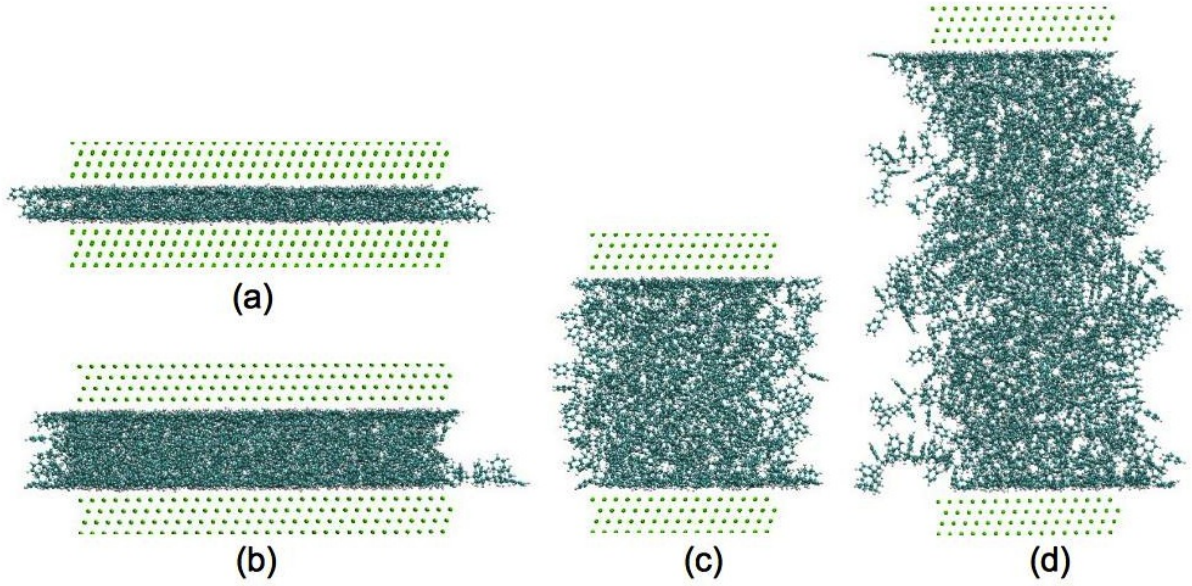

Figure 3: Snapshots for the four systems (periodic boundary conditions applied on the molecule center-of-mass) studied a) S1 with 40 chains, b) S2 with 80 chains, c) S3 with 50 chains and d) S4 with 100 chains. Systems S1 and S2 are doubled along the x and y directions to improve statistics.

surface. It is clear that $< R_e^2 >^{\frac{1}{2}}$ of PS chains for all but the thinnest films have values which are very close to the bulk one. The situation for the S1 system is different. All three S1 films are under

Table 4: Properties of the four systems, including three independent simulations of system S1. The film density, ρ, is in units g cm^{-3}. The thickness, t, radius of gyration, $< R_g^2 >^{\frac{1}{2}}$, and end-to-end distance, $< R_e^2 >^{\frac{1}{2}}$, are given in nm.

	N	d (nm)	ρ (g/cm^3)	$< R_e^2 >^{\frac{1}{2}}$(nm)	$< R_g^2 >^{\frac{1}{2}}$(nm)
S1A	40	0.96	1.14	1.41	0.66
S1B	40	0.96	1.14	1.32	0.65
S1C	40	0.96	1.13	1.37	0.66
S2	80	1.90	1.15	1.59	0.69
S3	50	4.81	1.14	1.55	0.69
S4	100	9.82	1.11	1.54	0.69
B	50	–	0.97	1.54	0.69

particularly strong confinement since their thickness is smaller than the bulk value of $< R_e^2 >^{\frac{1}{2}}$. Consequently $< R_g^2 >^{\frac{1}{2}}$ and, more noticeably, $< R_e^2 >^{\frac{1}{2}}$ are smaller in these films. Although the density and value of $< R_g^2 >^{\frac{1}{2}}$ is similar in each S1 film, the value of $< R_e^2 >^{\frac{1}{2}}$ is less uniform.

How should we distinguish between the average R_e over all times and the average of a particular

time? This is the difference between instantaneous and running average data shown in next figure. <...> includes summation over t. To further study the fluctuations of the end-to-end distance, we show in Figure 4 the time evolution of the mean square $R_e(t)$ for all systems. With lines are the instantaneous values of R_e whereas with symbols are the running average data, averaged over the duration of the atomistic simulations. We see that for all but the thinnest system (S1), the average value of the end-to-end distance of the PS chains is very close to the value of the unperturbed bulk system. Small differences between the different systems are practically within error bars. In contrast, all the S1 films have clearly smaller values for the end-to-end distance and, furthermore, the three different S1 films also have different values. Clearly, for this system, the results do depend on the equilibration–annealing period (history of the sample). This is due to the fact that these strongly confined films are effectively frozen and their structures are rather dependent on set up and history, as will be shown later. Furthermore, the running average data shown that during the simulation runs R_e reach steady-state, time-independent values. The behaviour of the radius of gyration is qualitatively similar. Note that the this analysis is over the entire confined polymer system. The variation of the chain dimensions along z, are studied in the next subsection.

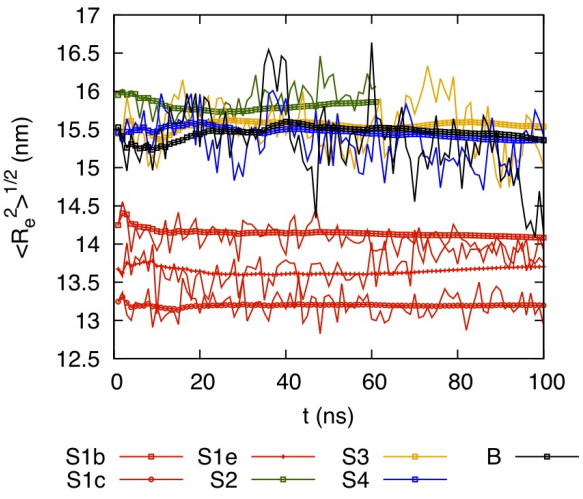

Figure 4: Time evolution of the end-to-end distance of the PS chains of all systems studied here.

The molecular density profiles, $\rho(z)$, of all systems are displayed in Figure 5a. The densities are based on the monomer centre-of-mass and are time-averaged. As expected, the density profiles

are symmetrical with respect to the centre of the film. As seen in the snapshots of the atomistic simulations in Figure 3, all films show a dense layer around 4 Å from the gold surface, labelled I. For the S4 system the density profile exhibits a characteristic oscillatory behaviour wherein a weak second peak, labelled II, can be discerned at a distance of around 10 Å from the Au surface. Similar density profiles with this characteristic oscillation have been observed in past simulations of polymer/solid interfaces with atomistic[? ? ?] as well as coarse-grained bead-spring models.[?] Add ref to Tinashe's PS/silica nanoparticle paper here?[?] In the middle region of systems S3 and S4, at distances beyond about 15–20 Å from the Au surfaces, ρ assumes a constant value equal to the density of the bulk PS 10-mer melt, $\rho = 0.97$ g cm^{-3}. In Figure 5b a close-up of the density profiles of the thinner systems, S1 and S2, are presented. All three independent S1 films are shown. Similar to S3, the S2 system shows one PS layer at the Au surface and the density in the middle of the film is very close to the bulk value. In contrast, the S1 films exhibit a qualitatively different behaviour with two strong adsorption layers and no bulk-like region.

Conformational properties

In this subsection, we first present data on segmental level ordering by analysing the local bond orientation tendencies induced by the Au surfaces. In general, the orientation of a molecule can be quantified by calculating the second rank order parameter. For an arbitrary vector along the molecule, $\vec{v}$, this is defined as

$$P_2 = \frac{3}{2}\left\langle \cos^2\theta \right\rangle - \frac{1}{2} \tag{3}$$

where θ is the angle of the vector $\vec{v}$ with the z coordinate axis (in this case normal to the surface). The brackets denote the ensemble average of all molecules in the system. The limiting P_2 values of -0.5 and 1.0 correspond to molecules oriented parallel and perpendicular to the surface, respectively. A value of 0.0 means that the molecules are randomly oriented.

We would like to distinguish between the local orientation of the backbone chains and of the side (phenyl) groups. Therefore, we analyze the local-bond orientation of the PS monomer by choosing vectors that connect a pair of carbons either at opposite sides of the phenyl ring or in the

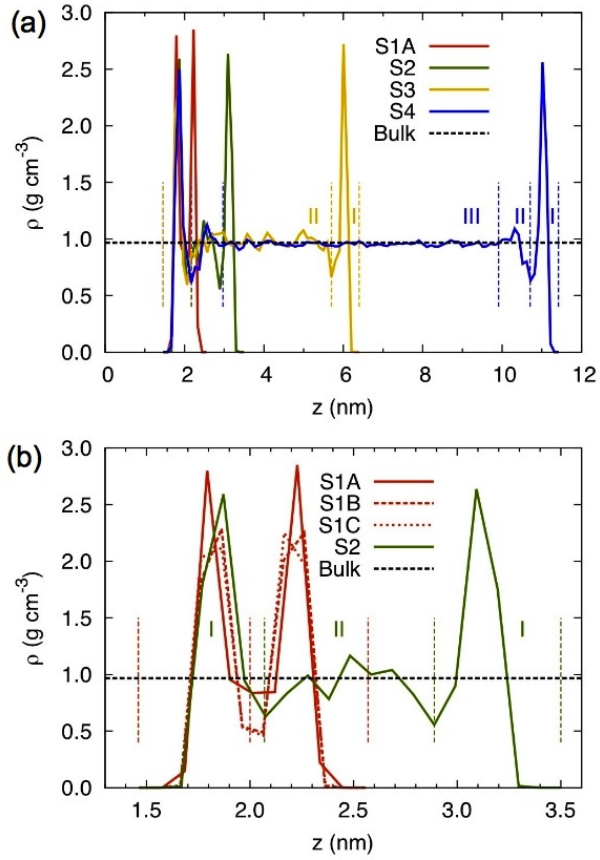

Figure 5: a) Monomer density for the four systems along the z-direction. b) Close-up of the S1 and S2 systems, including the three independent S1 films. In both graphs the vertical dashed lines correspond to the adsorption layers boundaries, which is used in the analysis.

neighbouring monomers along the backbone, as shown in Figure 6. Within the phenyl group there is a choice of three such atom pairs, of which only two are equivalent. The vector that includes the carbon atom attached to the backbone, v^{phb}, is not equivalent by symmetry to the other two vectors, v^{php}. Similarly for the backbone chain there are two choices of atom pairs: those connected to the phenyl group, v^{bbp}, and those that are not, v^{bbb}.

Figure 6: A PS 3-mer chain, with the backbone C atoms highlighted in lilac for clarity and showing the vectors used for bond order analysis.

Graphs showing the variation along z of the bond order parameters are shown in Figure 7. The data is analysed along the direction of confinement, z, by dividing the space into bins separated by

parallel *x*-*y* planes, and then averaged to take into account the symmetry of the film. For all the vectors and systems, the bond order parameters attain negative values of almost -0.5 at around 1–2 Å away from the Au surfaces, indicating the strong tendency of the backbone and phenyl groups to orient parallel to the surface plane. The P_2 then increase to a peak at ≈3–5 Å from the surface, although the height and position depends on the vector and system under consideration. For systems S2–S4 the bond order parameter is zero in the centre of the film, indicating random orientation, whereas in system S1 the parameters do not reach a constant zero value in the centre. Despite the differences in the chain dimensions of the three S1 systems, there is little difference in average orientation in the films.

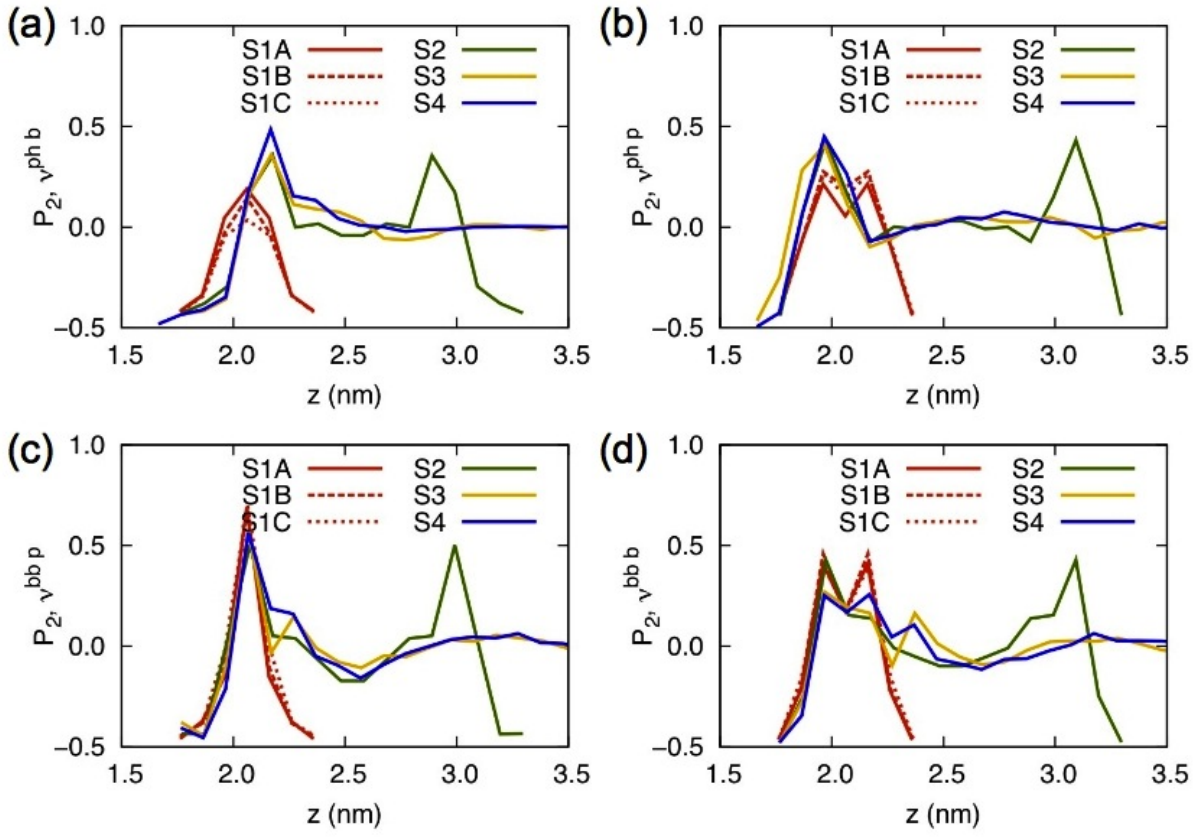

Figure 7: The variation of the bond order parameter with distance from the surface for all systems. The graphs correspond to the vectors a) v^{phb}, b) v^{php}, c) v^{bbp}, and d) v^{bbb}, as shown in Figure 6.

For the phenyl vector connected to the backbone chain, P_2^{phb}, systems S2–S4 have a peak value of 0.4–0.5 around 5 Å from the surface, shown in Figure 7a. This peak corresponds to the position

of the first minimum in the density profile i.e. the end of the first adsorption layer. The other phenyl vector, P_2^{php}, is shown in Figure 7b, and the peak is shifted towards the surface by around 2–3 Å. This shows that v^{php} has a slightly more random orientation close to the surface than v^{phb}. This is a consequence of the fact that the v^{php} are allowed to tilt around the v^{phb} 'axis', whereas v^{phb} is constrained by the backbone. A analogous behaviour is seen for P_2^{bbp} and P_2^{bbb}, shown in Figure 7c and d, respectively. By comparing P_2^{php} and P_2^{bbp} in Figure 7a and c, it is clear that the backbone peak value is higher than that of the phenyl vector, particularly in the case of the S1 films. This means that the orientation of the backbone is more strongly aligned perpendicularly to the surface at the density minimum.

It is easier to understand more about the orientational ordering by looking at the average values of the order parameters in the adsorption layers. An adsorption layer is defined as the distance between two consecutive minima in the density profiles, as shown in Figure 5. The data are shown in Table 5. The order parameter $P_{2\,\mathrm{ads}}^{\mathrm{phb}}$ of the first adsorbed layer, is negative for all systems, showing the tendency of molecules to be parallel to the surface plane. It is clear that this tendency is stronger in the S1–S3 systems with values of $P_{2\,\mathrm{ads}}^{\mathrm{phb}}$ between -0.22 and -0.31. The S4 system has a lower value of $P_{2\,\mathrm{ads}}^{\mathrm{phb}}$ than the other systems, indicating that it is slightly less ordered than the other systems. This is likely to be due to larger fluctuations and faster dynamics, as seen in Figure 4 in the following subsection. The bond order parameters in regions II and III in S2–S4 were also analysed but the magnitudes of all the order parameters are less than 0.1 indicating weak or random ordering. The analysis of $P_{2\,\mathrm{ads}}^{\mathrm{php}}$ shows a clear difference between the most confined films S1A–C and the other films S2–S4. For the S1 films the vectors have a slight tendency to be parallel to the surface, whereas in the large systems they show a weak preference for vertical orientation. Both backbone bond order parameters $P_{2\,\mathrm{ads}}^{\mathrm{bbp}}$ and $P_{2\,\mathrm{ads}}^{\mathrm{bbb}}$ are negative for all systems, again showing the tendency of molecules in the first adsorption layer to be parallel to the gold surface. The larger systems S2–S4 have more strongly negative values than S1A–C films. In particular, the orientation of the bond vector $P_{2\,\mathrm{ads}}^{\mathrm{bbb}}$ is almost random in the S1 films but has quite a strong parallel orientation in S2–S4.

Table 5: Average value of the $P_2(\cos(\theta))$ bond order parameters in the adsorption layer of each film for the vectors shown in Figure 6. SHOULD WE SHOW II and III (numbers in comments in tex file)?

Atoms	Region	$P_{2\,\mathrm{ads}}^{\mathrm{phb}}$	$P_{2\,\mathrm{ads}}^{\mathrm{php}}$	$P_{2\,\mathrm{ads}}^{\mathrm{bbp}}$	$P_{2\,\mathrm{ads}}^{\mathrm{bbb}}$
S1A	I	−0.26	−0.10	−0.17	−0.06
S1B	I	−0.28	−0.09	−0.16	−0.04
S1C	I	−0.29	−0.09	−0.15	−0.05
S2	I	−0.31	+0.08	−0.26	−0.21
S3	I	−0.22	+0.08	−0.25	−0.19
S4	I	−0.16	+0.09	−0.29	−0.25

Next, we show information about the conformational properties of PS at the level of the entire chain. Changes in the shape of the chains can be analyzed in terms of a global descriptor of the overall polymer melt configuration, the so called conformation tensor C. This is defined as the second moment tensor of the end-to-end distance vector, $\vec{R}_{\mathrm{e}}$, of a polymer chain divided by one-third of its unperturbed mean-square end-to-end distance, $< R_{\mathrm{e}}^2 >_0$, averaged over all chains in the system

$$C_{\alpha\beta} = 3 \left\langle \frac{R_{\mathrm{e}\alpha} R_{\mathrm{e}\beta}}{< R_{\mathrm{e}}^2 >_0} \right\rangle \tag{4}$$

where α and β are the x, y and z components. Is this paragraph rewritten and not copied and pasted from somewhere? We have to be careful not to do this even if it is from one of your papers. Away from any boundary, the chain conformational statistics is unperturbed, to an excellent approximation, and, therefore, $\mathbf{C}$ reduces to the identity tensor, $\mathbf{C} = \mathbf{I}$. When the melt is subjected to a flow field over time scales shorter than or comparable to the longest relaxation time of the chains, or when the melt is found in the neighborhood of a boundary, chain shapes are distorted and $\mathbf{C}$ departs from its equilibrium isotropic value. In such a case, the non-zero components of $\mathbf{C}$ provide a measure of the orientation and/or extension of the chains along the three axes of the coordinate system.

The conformation tensor components, C_{xx}, C_{yy} and C_{zz}, were analysed as a function of the distance from the surface. The film was divided into layers along z, approximately 10 Å-thick, and within each layer, $\mathbf{C}$ is obtained as an ensemble average of individual molecular conformation

tensors over chains whose centers-of-mass lie in that layer. The results are then symmetrised along the z-direction and the in-plane components are averaged. Figure 8 displays the effect of the gold surface on the in-plane and perpendicular components for the S2–S4 systems. In all cases the in-plane components, $C_{\text{par}} = \frac{1}{2}(C_{xx}+C_{yy})$ are larger than 1.0 at the surface whereas the zz components are smaller. Therefore, the conformations are compressed along the z-direction and elongated along the surface plane, which means that the chains are lying along the surface. Quantitatively, $C_{zz} \approx 0.2$, which means that the surface affects the perpendicular component more that the in-plane components, which was observed experimentally? and in computer simulations.??? It can be also be seen from the S4 film that the conformation returns to the bulk value of 1.0 at around 2–3 nm, which is about twice the average bulk end-to-end distance of 1.54 nm.

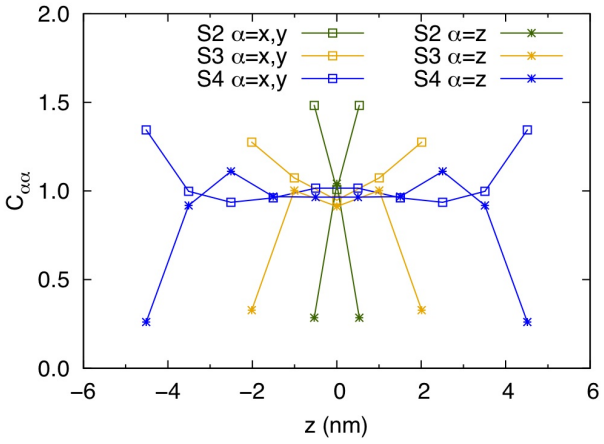

Figure 8: Variation of the conformation tensor components, C_{xx}, C_{yy} and C_{zz}, with z for all systems.

To further quantify these results and compare the various systems, the conformation tensor components of the adsorption layers for each system are given in Table 6. S3 and S2 exhibit similar conformational properties as S4. For the S1 films the results are more varied which is, again, a consequence of the dependence on system setup and the slow dynamics of these systems, which will be discussed in the next section.

We should also note that the studied systems shown a clear uniaxial anisotropy, studied through the Saupe matrix, S, (data not shown here) of the PS molecules along the z-direction. How do I get data from the Saupe matrix?

Table 6: Average value of the conformation tensors in the different regions of each film as labelled in Figure 5. $C_{\mathrm{par\,ads}}$ is the average in-plane value.

	Layer	$C_{\mathrm{par\,ads}}$	$C_{zz\,\mathrm{ads}}$
S1A	I	1.20	0.12
S1B	I	1.04	0.10
S1C	I	1.10	0.13
S2	I	1.64	0.20
	II	0.97	0.80
S3	I	1.64	0.13
	II	0.94	1.03
S4	I	1.39	0.15
	II	1.21	0.87
	III	0.95	1.02

Dynamical properties

In this section the effect of the confinement on the dynamics of the PS/Au films is analysed and discussed. A standard way to analyze the orientational dynamics of molecules is through time correlation functions of a vector **v**. Finally, we will present mean square diffusion and diffusion constants.

First, we consider the relaxation of the second-order bond order tensor P_2. As before, we consider the vectors v^{php}, v^{phb}, v^{bbp}, and v^{bbb} discussed in the previous subsection and shown in Figure 6. The time autocorrelation function of $\mathrm{P_2(t)}$ for all vectors in the 10-mer bulk system is shown in Figure 9a. The dynamics of the two backbone vectors is indistinguishable and from now on we only discuss v^{bbb}. As expected, the backbone dynamics is slower than the dynamics of the phenyl groups, which are less constrained. The two phenyl group vectors also have different dynamical behaviour, with the vector attached to the backbone, v^{phb}, being slower than v^{php}. Again, this is to be expected since the phenyl ring can spin/vibrate around the vector v^{phb}, whereas v^{phb} is constrained by the motion of the backbone. All the ACFs decorrelate around 10 ns. To obtain quantitative information from the ACFs we fit KWW functions of the form

blah (5)

to the data. The segmental relaxation times and exponents are presented in **??**.

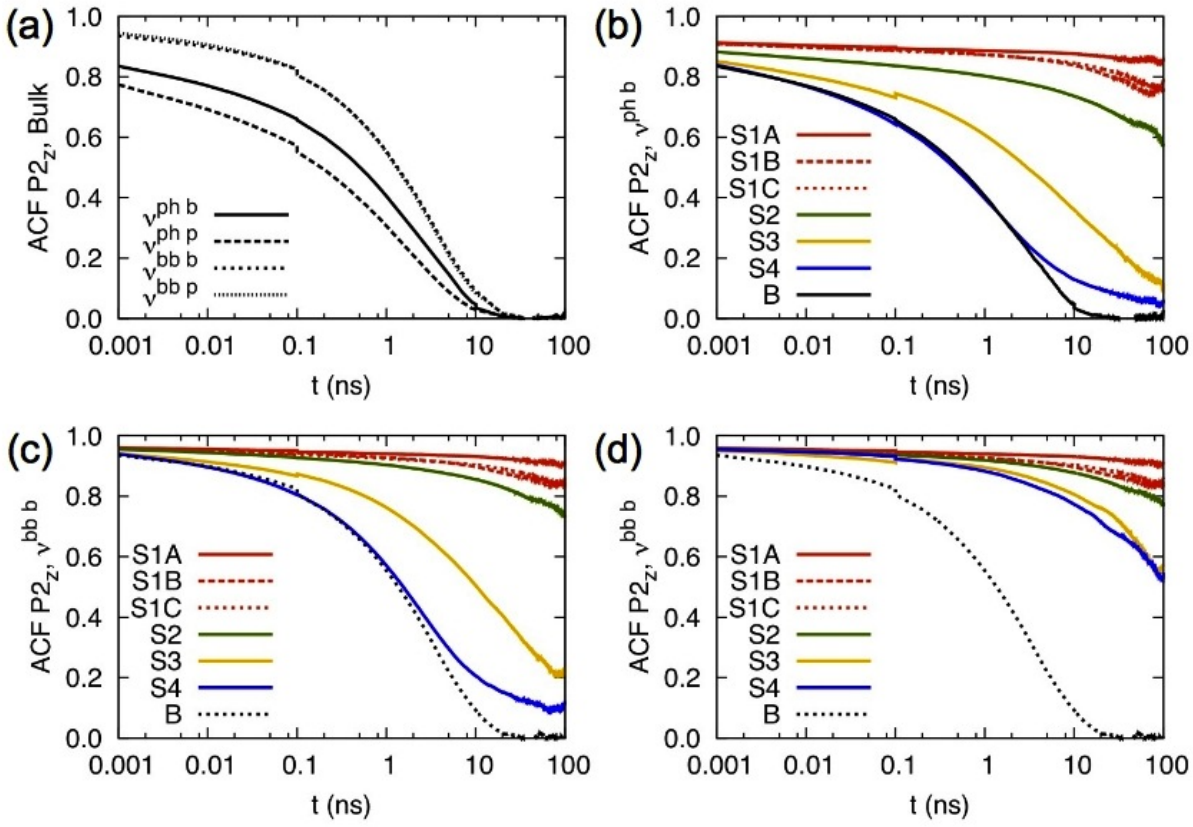

Figure 9: a) Time autocorrelation function of $P2$ in bulk for all the vectors shown in Figure 6. b) The ACF of v^{phb} for all systems c) The ACF of v^{bbb} for all systems. d) The ACF of v^{bbb} for the adsorption layer in all systems.

Figure 9b and c show the ACFs for the various systems for vectors v^{php} and v^{bbb}. For both vectors the trend in the same: increasing confinement slows the dynamics of the system. System S4 maintains bulk dynamics in the time regime up to around 1 ns. After this, the dynamics diverges from the bulk dynamics and appears to reach a plateau value of around 0.5–1.0, which is due to the much slower dynamics of the adsorption layer. For systems S1 and S2 the ACF is almost flat over the whole time range considered here and the system is virtually frozen and this explains the large differences in R_{g} and R_{e} seen earlier. Figure 9d shows the dynamics in the adsorption layer, labelled I in Figure 5, for systems S1–S4, compared to the bulk. All systems show a marked slowing down of the dynamics and none of the adsorption layers in any of the thin film systems

decorrelate over a time of 100 ns.

The translational dynamics of the confined PS short chains is analysed by calculating the mean square displacements (MSDs) of the monomer centers-of-mass. The results of this analysis are shown in Figure 10a. The bulk, as well as the two bigger systems (S3 and S4) exhibit, as expected, non-linear anomalous dynamics for short times (up to about 1 ns), and linear Fickean dynamics at longer times. The behaviour of the two smaller, more confined systems, is very different. Both S1 and S2 systems are practically frozen, i.e. there are only small vibrations and rotations (see Figure 10a), of about $3-6$ Å for S1 and 10 Å for S2.

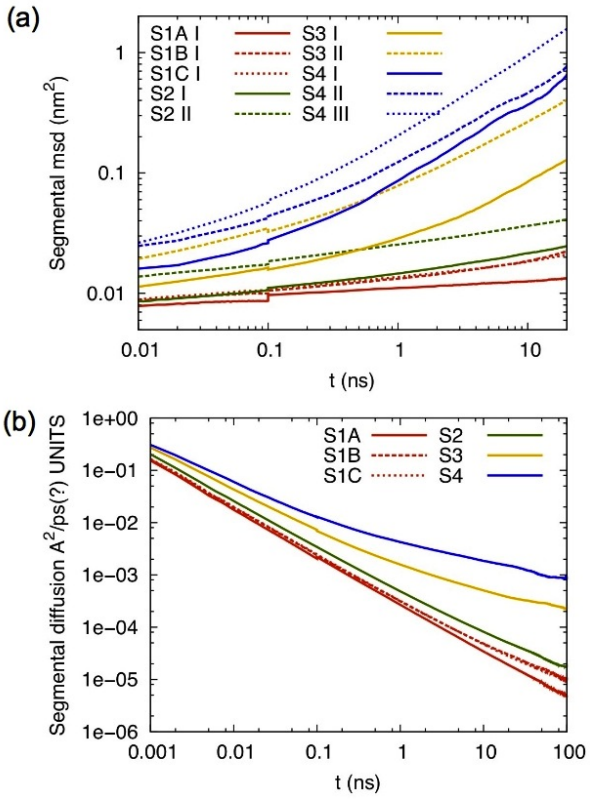

Figure 10: Translational centre-of-mass dynamics of all confined PS systems studied here: a) mean square displacements of monomer centre-of-mass b) Segmental diffusion.

The translational dynamics has also been analyzed in slices divided by planes parallel to the surface, corresponding to the regions shown in Figure 5. The MSD data in x-y are shown in Figure 10b. The S4 system has three regions, two adsorption layers and a bulk-like phase in the

middle, as shown in Figure 5. The first adsorption layer, I, is slowest.

The above behaviour is even more clear if we calculate the time-dependent x-y self-diffusion coefficient, defined as

$$D_{xy}(t) = \frac{\left\langle (R_{xy}(t) - R_{xy}(0))^2 \right\rangle}{4t}. \tag{6}$$

Values of $D_{xy}(t)$ for all the systems studied here are plotted in Figure 10b. As expected, the bulk system shows a time dependent value for the short times whereas it reaches a plateau value (at around $20-30$ ps) of about 0.25 ± 0.02 Å^2 ps^{-1}. The two thicker films (S4 and S3) exhibit qualitatively similar behaviour with plateau, time-independent, values of D_{xy} equal to 0.17 ± 0.03 Å^2 ps^{-1} and 0.08 ± 0.03 Å^2 ps^{-1} respectively. The molecules in both S2 and S1 systems show a constant decreasing $D_{xy}(t)$, which is to be expected since the molecules in these systems are practically frozen.

Summary and Conclusions

This research is a hierarchical dualscale study of short PS (10mer) chains confined between two gold surfaces at $T = 503$ K and $p = 1$ atm. A combination of DFT calculations and MD simulations were used. The DFT data were used to develop an accurate classical atomistic potential for the polymer with the surface. This interfacial potential was used in MD simulations for PS thin films confined between two parallel gold surfaces.

To obtain detailed chemical information at the interface, DFT calculations of ethane (representing the polymer backbone) adsorbed at different sites on the Au(111) surface were performed. The DFT calculations show that the adsorption of ethane on the gold surface is almost entirely due to vdW forces. The adsorption energies on the various surface sites and different molecular orientations were been examined and the minimum energy configuration is for ethane to lie with C–C bond parallel to the surface. The corresponding adsorption energy is 35.7 kJ mol^{-1}.

The derivation of a new, accurate classical pair molecule/surface force field, through parameterization of detailed DFT data, is a major part of this work. Using an optimization algorithm

based on simulated annealing, we obtained a set of non-bonded pair C–Au and H–Au parameters for ethane (the PS backbone) that accurately describe the detailed DFT data. We found that a Morse-type potential is a better choice than a Lennard-Jones potential for describing the DFT data. The Morse potential parameterisations give good agreement between the DFT and classical data for both flat and vertical molecular orientations. The potential for the phenyl group was developed in the same way in a previous publication.[?]

These interfacial potentials are used to describe the interaction between PS and gold in NpT molecular dynamics simulations. Four systems with different numbers of benzene molecules were studied using molecular dynamics and the PS film thicknesses ranged from 0.96–9.82 nm. For the thinnest system, three independent films were simulated. The density, structure and dynamics of the PS films were analysed.

All systems S1–S4, have a density peak, or adsorption layer, in the PS film at the gold surface, which is 2–2.5 times higher than the bulk density. An analysis of the conformation tensor shows that the chains in the adsorption layer tend to lie along the surface. Similarly, an analysis of the bond order parameter P_2 for showed that the phenyl and the backbone rings in the adsorption layer prefer to orient parallel to the surface. Only the S4 system shows a weak second adsorption layer but no strong orientation ordering was found in this layer. The density reaches a constant bulk value around 1.5–2 nm from the surface and the conformation tensor components return to a bulk value around 2–3 nm from the surface. For the three thinnest (S1) films the average end-to-end chain length was found to be smaller than for the other systems with average values ranging from 1.32–1.41 nm, compared to the bulk value of 1.54 nm. The average radius of gyration is also slightly smaller in these films. In this highly confined system the PS chains are practically trapped in a metastable configuration that depends strongly on the preparation of the model systems (history of the samples).

The time autocorrelation function of P_2 showed that the thinner the film the more the dynamics were suppressed. At 503 K, the thinnest films are almost completely frozen, whereas the dynamics of the 10 nm film is close to bulk dynamics. For all films, the autocorrelation function does not

completely decorrelate, which is due to the slower dynamics in the adsorption layer. How far from the surface are the dynamics affected?

Due to the slow dynamics at the surface, studies of polymer/solid systems are computationally challenging at the atomistic level due to the long time scales required for equilibration. Therefore, future work will be the development of a rigorous CG model for the polymer/surface interaction. This could then be used to study systems with higher molecular weights and the effect of confinement on the glass transition temperature.

Acknowledgement

The authors would like to thank Dominik Fritz(?) and Kostas Daoulas(?) - VH: Good choice for critical reading of the manuscript. Funding was provided by the DFG SPP 1369 Priority Program. This work was partially supported by the FP7-REGPOT-2009-1 project "Archimedes Center for Modeling, Analysis and Computation".